An Active-damping-compensated Magnetorheological Elastomer Adaptive Tuned Vibration Absorber

ZHENBANG XU, XINGLONG GONG,* GUOJIANG LIAO AND XIANMIN CHEN

CAS Key Laboratory of Mechanical Behavior and Design of Materials, Department of Modern Mechanics, University of Science and Technology of China, Hefei 230027, China

ABSTRACT: This article presents the development of an active-damping-compensated magnetorheological elastomer (MRE) adaptive tuned vibration absorber (ATVA). The principle and the vibration attenuation performance of the proposed active-damping-compensated ATVA were theoretically analyzed. Based on the analysis, a prototype was designed and manufactured. Its dynamic properties and vibration attenuation performances were experimentally investigated. The experimental results demonstrated that the damping ratio of the prototype was significantly reduced by the active force. Consequently, its vibration attenuation capability was significantly improved compared with a conventional MRE ATVA.

Key Words: adaptive tuned vibration absorber, magnetorheological elastomer, active damping compensated, velocity feedback, vibration attenuation performance.

INTRODUCTION

TUNED vibration absorbers (TVAs) are widely used in industries to suppress undesired vibrations of some machines excited by harmonic forces. However, the TVA is only effective over a considerably narrow frequency range. As the excitation frequency varies, the vibration attenuation effect of the TVA decreases or even collapses because of mistuning. This problem limits many applications of the TVAs. One solution to this problem is to develop adaptive tuned vibration absorber (ATVA).

In principle, the ATVA improves the vibration attenuation performance by adjusting its resonant frequency in real time to track the excitation frequency. A variety of ATVAs have been proposed. The major types include mechanical ATVAs, electromagnetic ATVAs, and ATVAs using controllable new materials. The mechanical ATVA achieves the variable stiffness element through mechanical mechanisms (Franchek et al., 1995; Nagaya et al., 1999; Kidner and Brennan, 2002; Bonello et al., 2005). This kind of ATVA has some advantages of good stability, long-life running, and easily available material. However, it usually needs a large redundant mass to adjust its stiffness, and the adjusting speed is slow. The electromagnetic ATVA uses a variable magnetic spring controlled by current as the stiffness element (Liu and Liu, 2006). It can

tune quickly but uses more energy. The ATVAs using controllable new materials have potential to solve these problems; therefore, they have been investigated widely. Currently, the controllable new materials used in ATVA mainly include shape memory alloy (Rustighi et al., 2005) and magnetorheological elastomer (MRE) (Holdhusen and Cunefare, 2004; Deng et al., 2006; Lerner and Cunefare, 2008).

MRE is a kind of smart material, whose modulus can be controlled rapidly, continuously, and reversibly by applying an external magnetic field. This characteristic makes it used as the smart springs of the ATVA. In the developed MRE ATVAs, the MRE can work in shear mode (Deng et al., 2006), squeeze mode (Holdhusen and Cunefare, 2004), or compression mode (Lerner and Cunefare, 2008). Lerner and Cunefare (2008) also investigated the vibration absorption characteristics of these working modes. Nevertheless, the vibration attenuation effects of these MRE ATVAs are unsatisfactory because of the large damping of the MRE. For the ATVA, the smaller the damping is, the higher the vibration attenuation performance can be achieved (Brennan, 1997; Sun et al., 2007). The damping is caused by the combining defect between the magnetic particles and the matrix in the MRE, which is difficult to be removed from material itself (Chen and Gong, 2008). Therefore, it is necessary to find other effective methods to improve the vibration attenuation performance of the MRE ATVA, in addition to reducing the damping of the MRE materials. Ni et al. (2009) designed a dynamic stiffness-tuning absorber with MRE. The device can equivalently reduce the damping by using the enhanced effect of squeeze strain

*Author to whom correspondence should be addressed.
E-mail: gongxl@ustc.edu.cn
Figures 2–4 and 6–12 appear in color online: http://jim.sagepub.com

of the MRE in the direction of particles chain. However, the method is too complicated to be used practically.

The purpose of this article is to improve the vibration attenuation performance of the MRE ATVA with an active control. In this research, the active damping compensation is used to reduce the adverse effects of the damping on the vibration attenuation performance. An active-damping-compensated MRE ATVA was designed and manufactured. Its feasibility and effectiveness was verified by experimental studies. This article is split into four sections. Following the introduction section, the principle and the vibration attenuation performance of the developed active-damping-compensated ATVA are analyzed in section 2. Section 3 describes the prototype of the active-damping-compensated MRE ATVA and the evaluation experiments of the dynamic properties and the vibration attenuation performance. The conclusions are summarized in the final section.

THE PRINCIPLE OF THE ACTIVE-DAMPING-COMPENSATED ATVA

Control Strategy

The control strategy of the active-damping-compensated ATVA is deduced based on the analysis of the control strategy of the active–passive vibration absorber. A single-degree-of-freedom primary system with an active–passive vibration absorber is depicted in Figure 1. The active element is placed between the absorber mass and the primary system. For the convenience of analysis, the system is divided into three parts as follows: the primary system (part 1), the spring and damping of the active–passive vibration absorber (part 2), and the absorber mass (part 3). In Figure 1, f_1 is the force applied to part 1 from part 2; f_2 is the force applied to part 2 from part 3; f_{act} is the active force; m_{p}, c_{p}, and k_{p} are the mass, damping, and stiffness of the primary system, respectively; m_{a}, c_{a}, and k_{a} are the mass, damping, and stiffness of the active–passive vibration absorber, respectively; x_{p} and x_{a} are the displacements of the primary system and the absorber mass, respectively; and f is the harmonic excitation force applied on the primary system.

The equations describing this system are as follows:

$$f + f_1 = z_{\mathrm{p}} x_{\mathrm{p}} \qquad -f_1 - f_{\mathrm{act}} = z_{\mathrm{k}}(x_{\mathrm{p}} - x_{\mathrm{a}}),$$
$$f_2 + f_{\mathrm{act}} = z_{\mathrm{k}}(x_{\mathrm{a}} - x_{\mathrm{p}}) \qquad -f_2 = z_{\mathrm{m}} x_{\mathrm{a}} \tag{1}$$

where $z_{\mathrm{p}} = -m_{\mathrm{p}}\omega^2 + j\omega c_{\mathrm{p}} + k_{\mathrm{p}}$ $z_{\mathrm{k}} = k_{\mathrm{a}} + j\omega c_{\mathrm{a}}$ $z_{\mathrm{m}} = -m_{\mathrm{a}}\omega^2$ are the impedances of three parts, respectively. ω is the frequency of the harmonic excitation force f. By solving Equation (1), the displacement x_{p} can be derived as
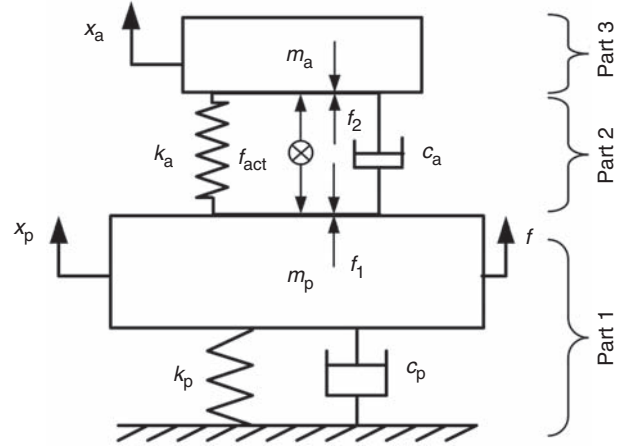
Figure 1. A single-degree-of-freedom primary system with an active–passive vibration absorber.

follows:

$$x_{\mathrm{p}} = \frac{z_{\mathrm{k}} x_{\mathrm{a}} + z_{\mathrm{m}} x_{\mathrm{a}} - f_{\mathrm{act}}}{z_{\mathrm{k}}}. \tag{2}$$

Setting x_{p} to zero gives the following:

$$f_{\mathrm{act}} = (k_{\mathrm{a}} - m_{\mathrm{a}}\omega^2) x_{\mathrm{a}} + j\omega c_{\mathrm{a}} x_{\mathrm{a}} = (k_{\mathrm{a}} - m_{\mathrm{a}}\omega^2) x_{\mathrm{a}} + c_{\mathrm{a}}\dot{x}_{\mathrm{a}}. \tag{3}$$

Equation (3) is the control strategy of the active resonator absorber (Filipovic and Schroder, 1998; Jalili and Knowles, 2004). From this equation, the active force of the active resonator absorber consists of two parts as follows: displacement feedback and velocity feedback. The action of the displacement feedback is to tune the equivalent resonant frequency of the absorber, and the action of the velocity feedback is to counteract the damping force of the absorber. In fact, the active resonator absorber is similar to an auto-tuning un-damping vibration absorber, whereas the performance is realized only by the active force (Sun et al., 2007). With further deduction, the f_{act} can be stated as follows:

$$f_{\mathrm{act}} = \sqrt{(k_{\mathrm{a}} - m_{\mathrm{a}}\omega^2)^2 + (\omega c_{\mathrm{a}})^2}\, e^{j\theta} x_{\mathrm{a}}$$
$$= \sqrt{(k_{\mathrm{a}} - m_{\mathrm{a}}\omega^2)^2 + (\omega c_{\mathrm{a}})^2}\, x_{\mathrm{a}}(t - \tau), \tag{4}$$

where

$$\tau = -\frac{1}{\omega}\theta = \frac{1}{\omega}\left\{\tan^{-1}\left[\frac{c_{\mathrm{a}}\omega}{m_{\mathrm{a}}\omega^2 - k_{\mathrm{a}}}\right] + 2(N-1)\pi\right\},$$
$$N = 1, 2, \ldots$$

Equation (4) is the control strategy of the delayed resonator (Olgac and Hansen, 1995; Olgac and Jalili, 1998). Because this control strategy comes from
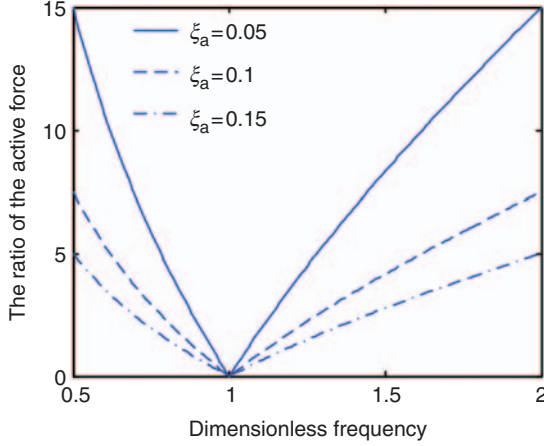
Figure 2. *The ratios of the active force with different damping ratios.*

Equation (3), it is the same as the control strategy of the active resonator absorbers in nature. The delayed resonator can also be considered as an auto-tuning undamping vibration absorber, whereas the performance is realized by a displacement delaying feedback.

For the active resonator absorbers and the delayed resonators, the ratio of the force to tune frequency and the force to counteract damping force can be written as follows:

$$\gamma = \left| \frac{(k_a - m_a\omega^2)x_a}{j\omega c_a x_a} \right| = \left| \frac{1}{2j\xi_a}\left(\frac{1}{\Omega_a} - \Omega_a\right) \right|, \quad (5)$$

where $\xi_a = c_a/(2\sqrt{k_a m_a})$ is the damping ratio of the absorber, and $\Omega_a = \omega/\omega_a = \omega/(\sqrt{k_a/m_a})$ is the dimensionless frequency. The ratios γ with different damping ratios are presented in Figure 2. It is shown that the active force to tune frequency is much larger than one to counteract damping force except a narrow band near the resonant frequency of the absorber ω_a. In addition, the curve with a small damping ratio is above that with a large damping ratio, which means the active control energy is mainly used to tune the equivalent resonant frequency of the absorber when the damping is small.

The idea of the active-damping-compensated ATVA is inspired by the fact that the total needed active force will be reduced greatly if the active force to tune the frequency can be removed. By using the variable stiffness spring to adjust the resonant frequency, the device does not need the active force to tune frequency. The control strategy of the stiffness of the active-damping-compensated ATVA is:

$$k_a = m_a\omega^2. \quad (6)$$

To counteract the damping force, the control strategy of the active force is:

$$f_{act} = g\dot{x}_a = \lambda c_a \dot{x}_a, \quad (7)$$

where g is the feedback gain and λ is the proportionality coefficient. As stated previously, the control principle of the active-damping-compensated ATVA can be written as follows:

$$\begin{cases} k_a = m_a\omega^2 \\ f_{act} = g\dot{x}_a \end{cases}. \quad (8)$$

Vibration Attenuation Performance of the Active-damping-compensated ATVA

From Equations (1) and (8), the driving point mobility of the primary system with an active-damping-compensated ATVA attached can be obtained as follows:

$$H_1 = \frac{x_{p\text{-with}}}{f} = \frac{1}{\frac{z_m z_k}{z_m - z_g + z_k} + z_p}$$

$$= \frac{1}{\frac{-m_a\omega^2(m_a\omega^2 + j\omega c_a)}{-j\omega g + j\omega c_a} - m_p\omega^2 + k_p + j\omega c_p}, \quad (9)$$

where $z_g = j\omega g$.

When the active-damping-compensated ATVA is removed, the driving point mobility of the primary system can be written as follows:

$$H_2 = \frac{x_{p\text{-without}}}{f} = \frac{1}{-m_p\omega^2 + j\omega c_p + k_p}. \quad (10)$$

The vibration attenuation effect is defined as the ratio of the driving point mobility of the primary system with and without active-damping-compensated ATVA attached, the dB expression of the effect is:

$$\beta = 20\log\left(\frac{H_1}{H_2}\right)$$

$$= 20\log\left\{ \frac{\mu\left[-1 + 2j\xi_p\frac{1}{\Omega_p} + \left(\frac{1}{\Omega_p}\right)^2\right]}{\frac{-\Omega_p\left(1 + 2j\xi_a\frac{1}{\Omega_p}\right)}{2j\xi_a(1-\lambda)} + \mu\left[-1 + 2j\xi_p\frac{1}{\Omega_p} + \left(\frac{1}{\Omega_p}\right)^2\right]} \right\}, \quad (11)$$

where $\Omega_p = \omega/\omega_p$ is the dimensionless frequency, $\mu = m_p/m_a$, and $\xi_p = c_p/(2\sqrt{k_p m_p})$ is the damping ratio of the primary system. Obviously, the small β represents the good vibration attenuation effect. When λ is equal to zero, Equation (11) becomes the expression of the vibration attenuation effect of the conventional ATVA.

The relationship between the effect β and dimensionless frequency Ω_p is demonstrated in Figure 3. As shown in this figure, the shape of the curves with $\lambda > 0$ is similar
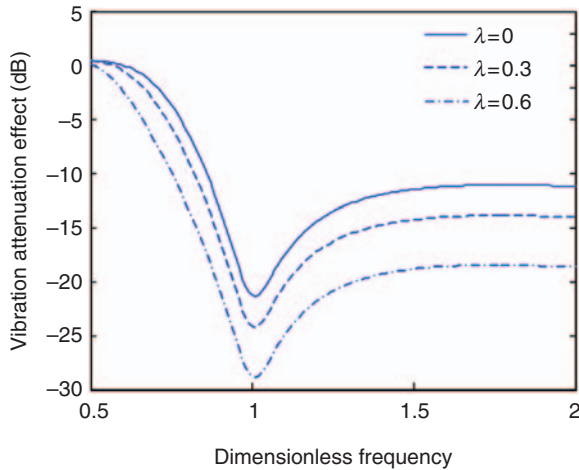
Figure 3. *Vibration attenuation effect with different feedback gains, $\mu = 4$, $\xi_p = 0.06$, and $\xi_a = 0.1$.*

to that with $\lambda = 0$, and the greater the gain is, the better the effect is. The results demonstrate that the action of the active force is to counteract the damping force, and it can counteract more damping force when the feedback gain is greater.

The damping force f_d of the vibration absorber is:

$$f_d = c_a(\dot{x}_a - \dot{x}_p).$$

For the vibration absorber, $|\dot{x}_a| \gg |\dot{x}_p|$ stands, so the f_d can be written approximately as follows:

$$f_d \approx c_a \dot{x}_a.$$

The action of the active force is to counteract the damping force of the system. However, if λ is larger than 1, the active force f_{act} becomes larger than the damping force f_d, which will cause the equivalent damping of the system to become negative. The negative damping will make the system unstable. Therefore, λ should be controlled to be smaller than 1 for maintaining the stability of system.

THE ACTIVE-DAMPING-COMPENSATED MRE ATVA

Structure and Working Principle

A prototype of the active-damping-compensated MRE ATVA was built. Figure 4(a) shows a scheme of the prototype, and Figure 4(b) shows a photograph of the prototype. The prototype uses two MRE elements that work in shear mode as the smart spring. The magnetic field is created by two coils, and the field strength is controlled by the coil current. The absorber mass of the prototype is an enclosed configuration, which makes the best use of the space and reduces the size of the prototype. The coils and the magnetic conductor are fixed to
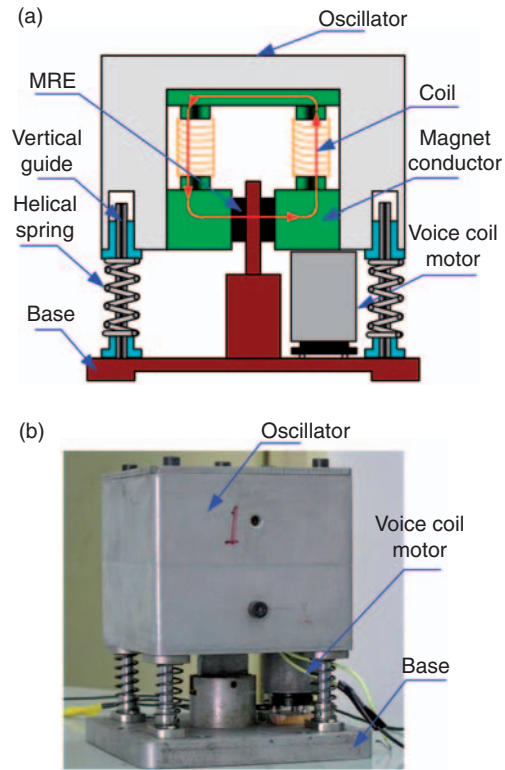
Figure 4. *The active-damping-compensated MRE ATVA: (a) scheme, and (b) photograph.*

the absorber mass, and they are part of the effective absorber mass of the prototype. This configuration can reduce the redundant mass, which degrades the vibration attenuation. The stiffness element of the prototype consists of smart spring elements with MRE and four helical springs. The action of the helical springs is to bear the weight of the absorber mass to prevent damage to the MRE elements caused by overlarge strain. The absorber mass is guided in the direction of vibration by four vertical guides that are fixed to the base.

The MRE's shear modulus depends on the field strength. By adjusting the field strength as well as the coil current, the effective stiffness and hence resonant frequency of the prototype can be adjusted. The active force is provided by a small voice coil motor. The motor consists of a magnet and motor coil. The magnet is fixed to the absorber mass, and the motor coil is fixed to the base. When a current flows through the motor coil, an ampere force will be generated between the magnet and the motor coil. The amplitude and direction of the force can be controlled by the current.

The control strategy of the active force is shown as Equation (7). The control system consists of four main parts as follows: accelerometer, charge amplifier that has an integrator, signal conditioning circuit, and power amplifier. The acceleration signal of the absorber mass measured by an accelerometer is integrated for one
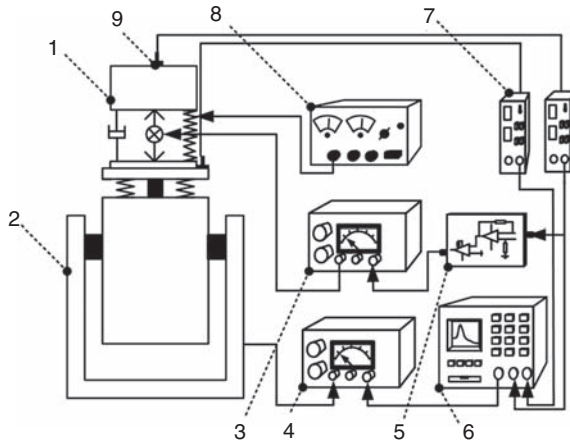
Figure 5. *The system for evaluation of the frequency shift property. 1. Prototype, 2. vibration table, 3. power amplifier of the voice coil motor, 4. power amplifier of the vibration table, 5. signal conditioning circuit, 6. signal analyzer, 7. charger amplifier, 8. DC power, and 9. accelerometer.*

time by a charge amplifier to obtain the velocity signal. The amplitude and zero of the velocity signal are adjusted by the signal conditioning circuit. Following the signal conditioning circuit, a power amplifier is used to change the control voltage signal to current signal to drive the voice coil motor. The total feedback gain of the system is the product of the gains of four parts.

Experimental Evaluation of Frequency-shift Property

The system for evaluation of the frequency-shift property of the prototype is shown in Figure 5. The prototype was fixed on a vibration table. The signal analyzer (model: Signal Calc ACE DP240, Data Physics Corp.) provided an excitation signal to drive the system via a power amplifier. Two accelerometers (model: CA-YD, manufactured by Sinocera Piezotronics Inc., China) were placed on the absorber mass and the vibration table to measure their responses, respectively. The measured signals were integrated for one time at charge amplifiers (model: YE5858A, manufactured by Sinocera Piezotronics Inc., China) to obtain the velocity signal.

The velocity signal of the absorber mass is used as control signal of the voice coil motor, and it was also sent to the signal analyzer as the output signal of the prototype. The velocity signal of the vibration table was sent to the signal analyzer as the input signal of the prototype. With the input and output signals, the transmissibility, relating the velocity of the absorber mass to the velocity of the vibration table, can be obtained by using fast Fourier transform (FFT) analysis. The peak position of the transmissibility curve is the resonant frequency of the prototype. The damping ratio can be computed by using the half power bandwidth method with the transmissibility curve.

The field current was supplied by an external DC power. For each current setting, swept-frequency signal excitation was applied and the transmissibility was measured. If the voice coil motor does not work, the prototype becomes a conventional ATVA. Figure 6(a) shows the transmissibility curves of the conventional ATVA, and Figure 6(b) shows the transmissibility curves of the active-damping-compensated ATVA. It can be seen that the transmissibility curves all move rightward with the increase in the current. Moreover, the peaks of the curves of the active-damping-compensated ATVA are higher and sharper than that of the conventional ATVA. The results demonstrate that the active-damping-compensated ATVA has smaller damping ratio than conventional ATVA. That is, the active force exerts positive effects on counteracting damping force. In this experiment, the chosen feedback gain is 100.

Figure 7(a) shows the relationship of the resonant frequency versus the coil current. The resonant frequency of the conventional ATVA increases from 29.94 Hz at 0 A to 47.23 Hz at 0.8 A, whereas the frequency-shift range of the active-damping-compensated ATVA is from 28.75 to 44.56 Hz. The resonant frequency of the active-damping-compensated ATVA is smaller than that of the conventional ATVA under a certain current because of the larger vibration amplitude caused by smaller damping (Deng and Gong, 2007; Zhang and Li, 2009). The damping ratios obtained by using the half power bandwidth method are shown in Figure 7(b). It is shown that the active force reduced the average damping ratio to ∼0.06 from ∼0.16.

Experimental Evaluation of the Vibration Attenuation Performance

Figure 8 shows the schematic of the experimental setup for evaluation of the vibration attenuation performance of the active-damping-compensated ATVA. The prototype was placed at the center of a clamped–clamped beam that was used as the primary system. Two accelerometers were used to measure the vibration acceleration signals of the beam and the absorber mass. The measured acceleration signals were integrated by charge amplifiers to obtain velocity. A programmable current source control signal and an AC voltage signal to control the voice coil motor were obtained by using these velocity signals as the input to the controller. As shown in Figure 8, the vibration absorber has two control systems altogether. One is composed of the accelerometer fixed on the beam, the charger amplifier, the data collecting card, the upper computer, and the programmable current source. This control system is used to control the stiffness of the prototype. The control process of the stiffness is as follows. The measured velocity signal of the beam is converted to digital signal by a data
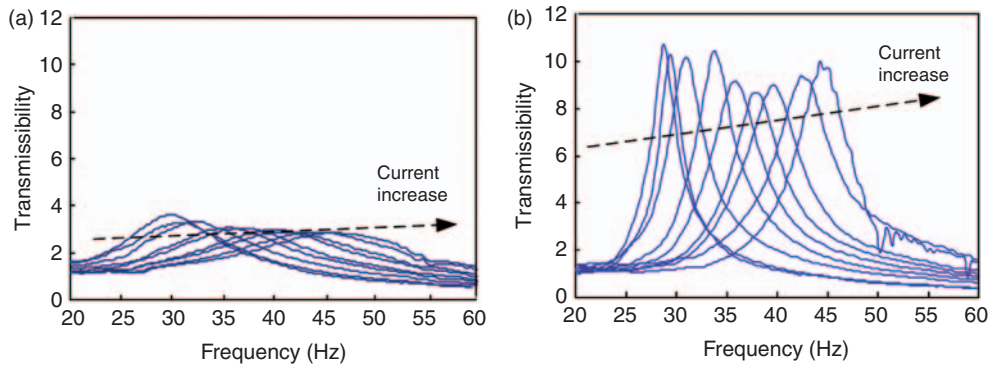
Figure 6. The transmissibility vs frequency at various currents: (a) conventional ATVA, and (b) active-damping-compensated ATVA.
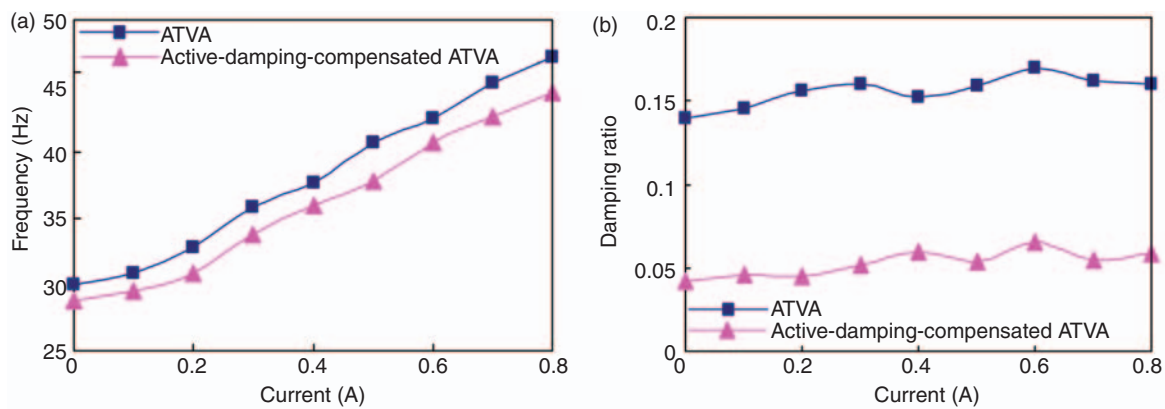
Figure 7. The experimental results of frequency shift property: (a) the resonant frequency vs applied current, and (b) the damping ratio vs applied current.
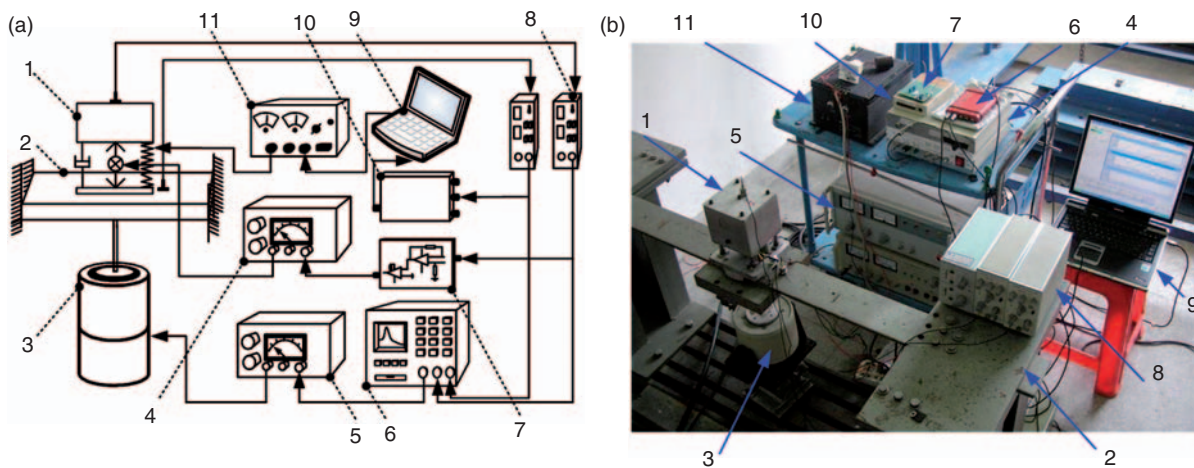
Figure 8. Experimental setup for investigating the vibration attenuation performance: (a) scheme, and (b) photograph.
1. Prototype, 2. clamped–clamped beam, 3. exciter, 4. power amplifier of the voice coil motor, 5. power amplifier of the exciter, 6. signal analyzer, 7. signal conditioning circuit, 8. charger amplifier, 9. upper computer, 10. data collecting card, and 11. programmable current source.

collecting card. The control program in the upper computer uses the digital velocity signal to obtain the dominant frequency by FFT analysis, and computes the corresponding current by using the tuning characteristic of the active-damping-compensated ATVA shown in Figure 7, then controls the programmable current source to supply the required current to adjust the stiffness of the vibration absorber. The other control system
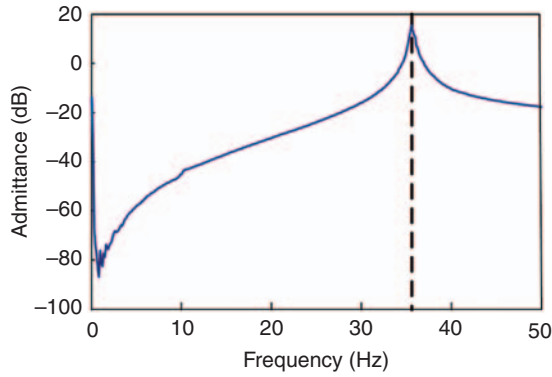
Figure 9. *The acceleration admittance of the beam.*
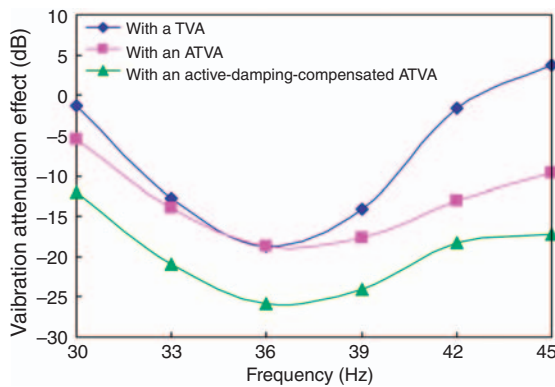
Figure 10. *Experimental results of the vibration attenuation effect in frequency domain.*

is composed of the accelerometer fixed on the absorber mass, the signal conditioning circuit, and the power amplifier of the voice coil motor. This control system is used to control the voice coil motor. Again, the control strategy is shown in Equation (7).

The clamped–clamped beam is made up of low carbon steel with a size of 930 mm × 100 mm × 11 mm. The pullback weight attached near the centre of the beam is 11 kg. Figure 9 shows the acceleration admittance of the beam measured by impedance head. As shown in this figure, the natural frequency of the beam is 36 Hz.

In the experiment, the system was excited with a series of single frequencies to approximate a swept sine excitation. The amplitude of the excitation force is 20 N, and the frequency range is 30–45 Hz. The vibration attenuation effect is represented by comparing the velocity of the beam with and without absorber. The effect is expressed as follows:

$$\gamma = 20 \log(V_{\text{with}}/V_{\text{without}}), \tag{12}$$

where V_{with} and V_{without} are the vibration velocity of the beam with and without absorber, respectively.

For harmonic vibration, the ratio of the velocities is equal to the ratio of the accelerations and the ratio of the displacements.

Figure 10 shows the experimental results of the vibration attenuation effect. If the prototype is not controlled and its resonant frequency is fixed at 36 Hz (the resonant frequency of the beam), it can be considered as a TVA. While the prototype is only controlled to trace the excitation force frequency, it can be looked as a conventional ATVA. As shown in Figure 10, for TVA, the best vibration reduction efficiency occurs at 36 Hz. When the excitation force frequency is apart from this frequency, the effect becomes bad. For ATVA, its vibration attenuation effect is equal to that of the TVA at 36 Hz, and it has better effect than TVA in the whole adjustable frequency band. Nevertheless, the superiority of the ATVA compared with the TVA is not evident because of the large damping. The active-damping-compensated ATVA has the best vibration attenuation effect. It resulted in a reduction of vibration of the beam by up to average 7 dB than the attenuation effect that can be achieved with the ATVA.

Figure 11 shows the experimental results of the vibration attenuation effect in time domain. In the entire process, both of the excitation frequency and the resonant frequency of the prototype were 30 Hz. During the time interval $0 \leq t \leq 2$, the voice coil motor did not work and the absorber worked as a conventional ATVA. At the moment of 2 s, the voice coil motor started to work and kept working until the end of the process. Figure 11(a) shows the velocity response of the absorber mass, which is used as the control signal of the voice coil motor. The signal amplitude with active force is slightly larger than that without active force. Figure 11(b) shows the response of the active force. The average amplitude of the force is about 2.8 N. Figure 11(c) shows the response of the beam during the process. The active force can reduce the amplitude of the vibration velocity by approximately a factor of two.

To investigate the control effect of the active-damping-compensated ATVA, some experiments were carried out. In the experiments, an excitation with single-step frequency change was supplied to the system. At the beginning, the system was excited at a frequency of 30 Hz and the absorber frequency was tuned to be this frequency. A few seconds later, the excitation frequency was increased in discrete steps up to 40 Hz then remained at 40 Hz until the end of the control process. The responses of the beam with a conventional MRE ATVA and the active-damping-compensated MRE ATVA attached are shown in Figure 12(a) and (b), respectively. The response experiences an increase caused by the change of the frequency and starts to decay as the current increases, eventually resumes the low level. It is noted that the active-damping-compensated ATVA achieves better vibration attenuation effect
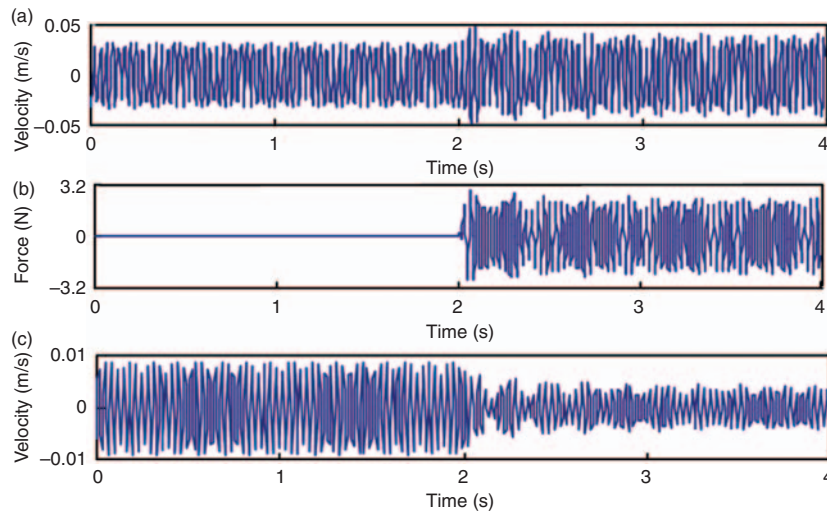
Figure 11. Experimental results of the vibration attenuation effect in time domain: (a) the response of the absorber mass, (b) the response of the active force, and (c) the response of the beam.
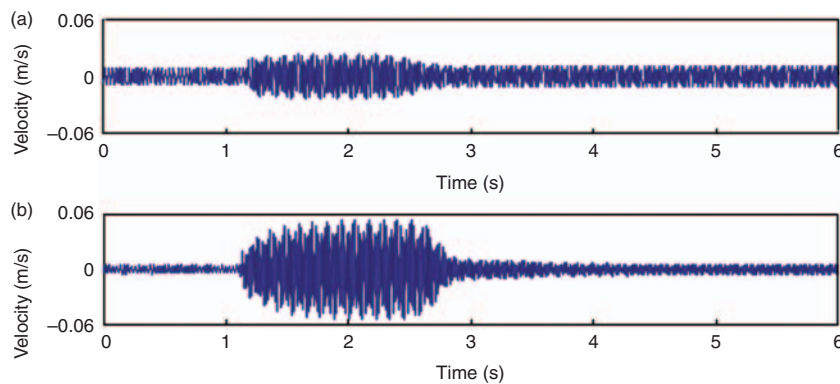
Figure 12. Comparison of the control effect with an conventional ATVA and an active-damping-compensated ATVA attached: (a) conventional MRE ATVA, and (b) active-damping-compensated MRE ATVA.

by counteracting the damping force when the tuned condition is maintained. During the transition segment, the response with an active-damping-compensated ATVA attached is larger than the one with a conventional ATVA attached because of the smaller damping. As shown in Figure 12, the time of the transient segment is about 1.5 s (the time for FFT analysis is more than 1 s) when the frequency is changed from 30 to 40 Hz, which means the active-damping-compensated ATVA can respond quickly. In many cases, the excitation frequency does not change frequently; therefore, the temporary increase of the response does not limit the application of the active-damping-compensated ATVA.

CONCLUSIONS

This article has described the principle, design, and testing of a novel active-damping-compensated MRE ATVA. The principle and the vibration attenuation effect of the active-damping-compensated ATVA were analyzed first in theory. The results show that the active-damping-compensated ATVA acts like a conventional ATVA with small damping. The larger the feedback gain is, the better the vibration attenuation is achieved. Based on the analysis, an active-damping-compensated MRE ATVA was developed. It consists of a MRE ATVA and a voice coil motor that is used to supply the active force. The experimental results of the frequency shift property indicated that the resonant frequency of the developed active-damping-compensated MRE ATVA varies from 28.75 Hz at 0 A to 44.56 Hz at 0.8 A, and the average damping ratio was reduced to 0.06 from 0.16 by the active force. Experimental studies were conducted to evaluate the vibration attenuation performance of the active-damping-compensated MRE ATVA on a clamped–clamped beam.

The results show that the active-damping-compensated MRE ATVA has improved vibration attenuation performance than conventional MRE ATVA.

REFERENCES

Bonello, P., Brennan, M.J. and Elliott, S.J. 2005. "Vibration Control Using an ATVA with a Variable Curvature Stiffness Element," *Smart Materials and Structures*, 14:1055–1065.

Brennan, M.J. 1997. "Vibration Control Using a Tunable Vibration Neutralizer," *Journal of Mechanical Engineering Science*, 211:91–108.

Chen, L. and Gong, X.L. 2008. "Damping of Magnetorheological Elastomers," *Chinese Journal of Chemical Physics*, 21:567–572.

Deng, H.X. and Gong, X.L. 2007. "Adaptive Tuned Vibration Absorber Based on Magnetorheological Elastomer," *Journal of Intelligent Material Systems and Structures*, 18:1205–1210.

Deng, H.X., Gong, X.L. and Wang, L.H. 2006. "Development of an Adaptive Tuned Vibration Absorber with Magnetorheological Elastomer," *Smart Materials and Structures*, 15:111–116.

Filipovic, D. and Schroder, D. 1998. "Bandpass Vibration Absorber," *Journal of Sound and Vibration*, 214:553–566.

Franchek, M.A., Ryan, M.W. and Bernhard, R.J. 1995. "Adaptive Passive Vibration Control," *Journal of Sound and Vibration*, 189:565–585.

Holdhusen, M.H. and Cunefare, K.A. 2004. "A State-switched Absorber Used for Vibration Control of Continuous Systems," *ASME Journal of Vibration and Acoustics*, 129:577–589.

Jalili, N. and Knowles, D.W.IV. 2004. "Structural Vibration Control Using an Active Resonator Absorber: Modeling and Control Implementation," *Smart Materials and Structures*, 13:998–1055.

Kidner, M.R.F. and Brennan, M.J. 2002. "Varying the Stiffness of a Beam-like Neutralizer Under Fuzzy Logic Control," *Journal of Vibration and Acoustics*, 124:90–99.

Lerner, A.A. and Cunefare, K.A. 2008. "Performance of MRE-based Vibration Absorbers," *Journal of Intelligent Material Systems and Structures*, 19:551–563.

Liu, J. and Liu, K. 2006. "A Tunable Electromagnetic Vibration Absorber: Characterization and Application," *Journal of Vibration and Acoustics*, 295:708–724.

Nagaya, K., Kurusu, A., Ikai, S. and Shitari, Y. 1999. "Vibration Control of a Structure by Using a Tunable Absorber and an Optimal Vibration Absorber Under Auto-tuning Control," *Journal of Sound and Vibration*, 228:773–792.

Ni, Z.C., Gong, X.L., Li, J.F. and Chen, L. 2009. "Study on a Dynamic Stiffness-tuning Absorber with Squeeze-strain Enhanced Magnetorheological Elastomer," *Journal of Intelligent Material Systems and Structures*, 20:1195–1202.

Olgac, N. and Hansen, B.H. 1995. "Design Considerations for Delayed-resonator Vibration Absorber," *Journal of Engineering Mechanics*, 121:81–89.

Olgac, N. and Jalili, N. 1998. "Modal Analysis of Flexible Beams with Delayed Resonator Vibration Absorber: Theory and Experiments," *Journal of Sound and Vibration*, 218:307–331.

Rustighi, E., Brennan, M.J. and Mace, B.R. 2005. "A Shape Memory Alloy ATVA: Design and Implementation," *Smart Materials and Structures*, 14:19–28.

Sun, H.L., Zhang, P.Q., Gong, X.L. and Chen, H.B. 2007. "A Novel Kind of Active Resonator Absorber and the Simulation on its Active Force," *Journal of Sound and Vibration*, 300:117–125.

Zhang, X.Z. and Li, W.H. 2009. "Adaptive Tuned Dynamic Vibration Absorbers Working with MR Elastomers," *Smart Structures and Systems*, 5:517–529.